
Article:
Rahim, S.A., Horoshenkov, K.V. orcid.org/0000-0002-6188-0369, Rongong, J. et al. (2 more authors) (2018) Epoxidized natural rubber for vibro-acoustic isolation. Polymer Testing, 67. pp. 92-98. ISSN 0142-9418

https://doi.org/10.1016/j.polymertesting.2018.02.018

Epoxidized natural rubber for vibro-acoustic isolation

Mahmud Iskandar Seth A Rahim[a], Kirill V Horoshenkov[a], Jem Rongong[a], Hamid Ahmadi[b], Judith Picken[b]

[a]Department of Mechanical Engineering, University of Sheffield, Velocity House, 3, Solly Street, Sheffield, South Yorkshire, S1 4DE, United Kingdom
[b]Engineering & Design, Tun Abdul Razak Research Centre, Brickendonbury, Hertford, Hertfordshire, SG13 8NL, United Kingdom

Corresponding author:
E-mail address: mibsetharahim1@sheffield.ac.uk (Mahmud Iskandar Seth A Rahim)

Abstract

The performance of an elastomeric vibro-acoustic isolation system is governed by the dynamic properties of the material under service temperature and frequency conditions. This paper investigates the effect of epoxidation level on the dynamic properties of Epoxidized Natural Rubber (ENR). Dynamic properties of natural rubber with 0, 25 and 50 mol% epoxidation levels were measured in simple shear over a range of temperatures and frequencies and a master curve for their dynamic properties was generated based on the time-temperature superposition principle. These master curves and the Cole-Cole plot of their dynamic properties shows that the epoxidation level does not affect the relationship between the storage modulus and loss modulus, but merely shifts the master curves for natural rubber along the frequency axis. These observations would be of value for designing a vibration isolation system with an optimum level of epoxidation to achieve the desired storage modulus (or loss modulus) at the given service conditions. A reduced temperature nomogram is presented for the prediction of appropriate epoxidation level required for such design purposes. The 5-parameter fractional derivative model by Pritz [J. Sound & Vib., 265, 935-952 (2003)] is fitted to the master curves for the complex dynamic modulus of natural rubber with different epoxidation levels.

Keywords:
Epoxidized natural rubber, Dynamic properties, Time-temperature superposition, Cole-Cole plot, Fractional derivative model

1. Introduction

Viscoelastic materials such as rubber are used extensively for vibro-acoustic isolation. The dynamic mechanical properties of these materials are dependent on the temperature and frequency. Therefore, it is necessary to test rubber compounds used in vibration and noise control applications in a range of environmental conditions and frequencies.

A chemically modified natural rubber (NR); Epoxidized Natural Rubber (ENR), is the focus of this study. ENR is produced by epoxidation of natural rubber with peracetic acid at the latex stage. A known percentage of its double bonds are reacted to form epoxide groups. As the epoxide groups are introduced, ENR shows a higher glass transition temperature (T_g) as compared to natural rubber by approximately 1°C for every mol% epoxidation [1]. This will strongly affect the dynamic mechanical properties of ENR [2].

ENR provides good resistance to oils and non-polar solvents, high damping at room temperature and low air permeability. These properties result from the high polarity of epoxide groups, which are randomly distributed along the natural rubber backbone [3, 4].

There are two commercial grades available for ENR which have different epoxidation levels: 25 mol% and 50 mol% [2], referred as ENR-25 and ENR-50. Rubber with any level of epoxidation can be developed under the right reaction conditions, which are mainly controlled by the peracetic acid concentration and epoxidation temperature [5].

A number of authors have reported on the dynamic mechanical properties of ENR. The materials investigated so far include blends of ENR and polymers with different T_gs such as polyvinyl chloride [6], ethylene vinyl acetate [7], natural rubber [8], polychloroprene [9] and ENR blends with ethylene propylene diene monomer rubber [10]. Materials consisting of ternary blends have also been reported such as ENR/polyvinyl chloride/chlorinated polyethylene [11] and ENR/natural rubber/cellulose [12]. Several studies on the performance of dynamic mechanical properties of ENR blends using different mixing approaches have been conducted. For example, Rooj et al. [13] developed a mixing technology based on an in-line electron induced reactive processing technique. Wang et al. [14] introduced wet masterbatch technique instead of using the traditional dry mixing method.

There is a relatively small amount of published work on dynamic mechanical properties of materials based on ENR alone as the main matrix. Furthermore, the effect of the epoxidation level on the dynamic properties of ENR has not been fully investigated. One particular study on the dynamic properties of ENR alone has been reported by Lu and Li [15]. They implemented an alternative approach in producing ENR with effective damping in a broad temperature range. It was shown that the application of a different crosslinking agent, phenolic resin, in the ENR matrix helps to achieve an effective damping with the loss factor of tan $\delta > 0.3$ and in the temperature range from -48°C to 100°C. However, the research they conducted focused only on a single epoxidation level of 40 mol%. The earlier work reported by Ahmadi et al. [16] has particularly addressed the effect of different epoxidation levels on the dynamic mechanical properties of ENR matrix. They have included a more interesting finding when they generated master shear modulus and loss factor curves of 0, 25 and 50 mol% epoxidation levels. The master curves obtained were found to be similar in shape.

In this study, the effect of different epoxidation levels on the dynamic properties of ENR as a single matrix was investigated for a wide range of temperatures and frequencies. Three types of natural rubber with different epoxidation levels of 0, 25 and 50 mol% were studied. The master curves of the rubbers were compared and nomogram relating the reduced frequency to the complex moduli at different temperatures was obtained. The influence of the epoxidation level on the relationship between the two dynamic moduli of the material was also studied using a Cole-Cole plot. Finally, the dynamic properties obtained were fitted by fitting the 5-parameter fractional derivative model by Pritz (Eq. 38 in ref. [17]) to the master curves for the complex dynamic modulus.

2. Experimental Procedures

2.1 Materials and Sample Preparation

Three types of natural rubber, SMR-CV60, ENR-25 and ENR-50 were obtained from the Malaysian Rubber Board. The basic details of the materials are shown in Table 1. All other ingredients were provided by Tun Abdul Razak Research Centre (TARRC), United Kingdom. All of the materials were commercial grade. The formulations used are given in Table 2. The formulations are denoted by R0, R25 and R50, where the numbers stand for the epoxidation level of the rubber.

Table 1
Rubber materials used in the experiments.

Material	Type	Characteristic	
		Epoxidation Level[2] (%)	Glass Transition Temperature, T_g[3] (°C)
Natural rubber	SMR-CV60[1]	0	-72.0
Epoxidized natural rubber	ENR-25	29.4	-45.5
	ENR-50	52.1	-25.1

[1] Standard Malaysian Rubber constant viscosity: grade 60
[2] as analysed by Proton Nuclear Magnetic Resonance (^{1}H NMR)
[3] estimated based on the epoxide levels analysed by ^{1}H NMR from relationship described by Davey and Loadman [1]

The materials were compounded on a laboratory 2-roll-mill machine maintained below 40°C. The rubber was loaded at the beginning of the compounding process. The other ingredients were mixed together and then loaded gradually to the 2-roll-mill. Finally, a smooth and uniform sheet was obtained. The compounding time was kept below 20 mins. The compounded natural rubber was left for 24 hours before being compression moulded into the rubber disc shaped of the double bonded shear test pieces for 20 minutes using an electrically heated hydraulic press at 150°C. The curing time was selected according to the crosslinking time at which 95% of cure has taken place

observed in the rheometer curve. The curve was analysed using a Monsanto Rheometer, MDR 2000.

Table 2
Formulations in parts per hundred of rubber (phr).

Ingredient	R0	R25	R50
SMR-CV60	100	-	-
ENR-25	-	100	-
ENR-50	-	-	100
Sulfur	2.5	2.5	2.5
Zinc Oxide	4	4	4
Stearic Acid	4	4	4
Wingstay L	1	1	1
CBS	1	1	1
PVI	0.3	0.3	0.3

The rubber pieces were bonded to stainless-steel surfaces during the curing process. The first step for bonding was to clean the stainless steel by dry sandblasting (air-blasting). Then, the stainless steel was immersed in acetone to remove the loose particles for 5 mins. Finally, a rubber-metal bonding system, Chemosil® 211 (primer) and Chemosil® 225 (covercoat) were applied to the stainless-steel surfaces which was to be bonded to the rubber pieces during the curing process. Drying time of 30 mins at room temperature for primer bonding agent was allowed before applying the covercoat bonding agent.

2.2 Dynamic Mechanical Characterisation

The dynamic properties of the three vulcanizates were measured using a Metravib DMA+1000 dynamic mechanical analyser. Tests were carried out over a frequency range of 0.1 to 170 Hz and a temperature range of -40 to 50°C with a dynamic strain of 0.1%. Double bonded shear test pieces (Fig. 1) were used. The nominal dimensions of the rubber discs were 10 mm in diameter and 2 mm thickness.

3. Results and Discussion

3.1 Effect of Temperature on the Dynamic Mechanical Properties

Fig. 2 illustrates the dependence of the storage modulus (G') as a function of temperature in the range of -40°C to 50°C for natural rubber with different epoxidation levels. These data were taken at 170 Hz excitation. This choice of frequency is the best to capture the development of the loss factor peak for the R0, R25 and R50 rubbers studied in this work.

It can be seen that all the materials exhibit high G' in the low temperature region. G'decreases with the increasing temperature. In this region the mobility of the polymer chains was increasing [12], so that a reduction in the material stiffness was expected. The storage modulus eventually converges for all three materials at around 50°C.

Fig. 3 shows the loss factor (tan δ) curves under the same conditions. This parameter gives a measure of the energy loss in the material due to the molecular rearrangement and internal friction in the natural rubber matrix. Above 5°C, tan δ, and therefore damping, increases with the increasing epoxidation level. Fig. 3 also indicates that T_g increases as the epoxidation level is increased, suggesting that the epoxide groups result in restricting movement the natural rubber chains. As a result, a higher temperature is needed to overcome the chain rigidity and interactions and allow rubbery behaviour.

3.2 Effect of Frequency on the Dynamic Mechanical Properties

The storage modules, G', of the three materials as a function of frequency and temperature is plotted in Figs. 4 to 6. It is frequency dependent, with its value increasing with frequency at all measured temperatures. However, at higher temperatures the storage modulus is relatively frequency independent. It becomes progressively more dependent on frequency as the temperature decreases. Well above the T_g, the molecules are free to move and experience relatively little resistance, so that a relatively low modulus can be observed. As a result, similar storage modulus values are obtained at high temperatures for all three compounds. However, as the temperature approaches the T_g, the frequency dependence of the properties becomes more pronounced, as shown in Figs. 4 to 6.

3.3 Time-Temperature Superposition

The isothermal curves plotted in Figs. 4 to 6 can be shifted along the frequency axis and storage modulus axis to obtain superposition. In practice, the dynamic mechanical properties of the rubber materials can be tested in a limited frequency range. However, it is possible to infer the dynamic mechanical properties of the rubber over a wider frequency range using the time-temperature superposition principle. The time-temperature superposition is expressed in the following equation [18, 19]:

$$G_{T_0}(a_T\omega) = \frac{\rho_0 T_0}{\rho T} G_T(\omega), \quad (1)$$

where G_{T_0} and G_T are the shear modulus at the reference temperature, T_0 and at a given temperature, T, respectively. a_T is the horizontal shift coefficient along the frequency axis, ω, while ρ_0 and ρ are the density of the material at T_0 and T, respectively, and:

$$\frac{\rho_0 T_0}{\rho T} = b_T, \tag{2}$$

b_T being the vertical shift coefficient.

The horizontal shift coefficient, a_T, is used to adjust the horizontal position of the isothermal curve along the frequency axis, whereas the vertical shift coefficient, b_T, is used to adjust the vertical position of the isothermal curve. The vertical shift coefficient, b_T, for all isothermal curves were determined using Eq. (2). It was assumed that the material density did not change significantly with temperature, so that the density value was kept constant.

The transition behaviour occurs in the range up to 100°C above T_g [20]. In this temperature range the frequency-temperature dependence of the dynamic properties of rubber can be inferred empirically. The approach suggested by Williams, Landel and Ferry (WLF) [21] expresses the shift factor, a_T, as the following:

$$\log a_T = -\frac{C_1(T - T_s)}{C_2 + T - T_s}. \tag{3}$$

Here, C_1 and C_2 are viscoelastic coefficients and T_s is the reference temperature estimated as:

$$T_s = T_g + 50°\text{C}. \tag{4}$$

Williams, Landel and Ferry suggested that the viscoelastic coefficients, C_1 = 8.86 and C_2 = 101.6. These values were selected based on the chosen reference temperature, T_s, of -30°C for polyisobutylene. If a different reference temperature, T_0 is chosen instead of T_s, then the new viscoelastic coefficients ${C_1}^0$ and ${C_2}^0$ are calculated based on the following equations:

$${C_1}^0 = \frac{C_1 C_2}{C_2 + T_0 - T_s} \tag{5}$$

and

$${C_2}^0 = C_2 + T_0 - T_s. \tag{6}$$

In this work, the chosen reference temperature, T_0, was 20°C, where the T_g of each rubber was estimated based on the epoxide levels analysed by nuclear magnetic resonance (NMR). The T_g of

R0, R25 and R50 rubbers were -72.0°C, -45.5°C and -25.1°C respectively. The new viscoelastic coefficients for R0, R25 and R50 at a reference temperature of 20°C are summarised in Table 3.

Table 3
The new viscoelastic coefficients for the reference temperature of 20°C.

Viscoelastic Coefficients	R0	R25	R50
$C_1{}^0$	6.27	7.69	9.31
$C_2{}^0$	143.6	117.1	96.7

The horizontal shift factor is calculated using:

$$\log a_T = -\frac{C_1{}^0(T - T_0)}{C_2{}^0 + T - T_0} \tag{7}$$

and their values for all rubbers are listed in Table 4.

3.4 Relationship of Dynamic Properties of Different Epoxidized Natural Rubbers

For a single homogenous polymer, plotting storage modulus, G' against the loss modulus, G'', known as Cole-Cole plot [22], would show the relationship between the two moduli without any information on the temperature and frequency at which the measurements were taken. The data collapses on an arc of a circle presenting the dynamic properties of the polymer from the rubbery to glassy phase. Fig. 7 shows this data for the natural rubber and ENR formulations tested. A full semicircle is not plotted as tests were not carried out at low enough temperatures approaching the glass transition temperature for these materials. The data for R0, R25 and R50 fall on a single arc suggesting that the epoxidation does not influence the relationship between storage modulus and loss modulus.

Fig. 8 shows the G' master curves for R25 and R50 rubbers shifted to the right to match the master curve for R0 rubber at reference temperature of 20ºC. This has been done by applying a multiplication factor to shift horizontally the curves for R25 and R50 rubbers. The multiplication factors for R25 and R50 rubbers were found to be 17 and 500, respectively. The same multiplication factors were applied to the master curves for G'' in Fig. 9.

It is also possible to shift the curves for R0 and R50 by altering the reference temperature from 20ºC to -3ºC for R0 and to 38ºC for R50 so that they overlap with the R25 curve at 20ºC. The temperature differences between the reference temperature for R25 (20ºC) and the new reference

Table 4
The horizontal shift coefficients for the reference temperature of 20°C.

Temperature (°C)	Horizontal shift coefficients, a_T		
	R0	R25	R50
-40	31551.529	-	-
-35	7786.905	-	-
-30	2231.669	-	-
-25	726.004	62785.932	-
-20	263.222	9731.792	-
-15	104.780	1892.968	-
-10	45.232	444.355	15379.298
-05	20.960	122.083	1761.166
00	10.336	38.315	267.527
05	5.385	13.470	51.181
10	2.946	5.221	11.849
15	1.683	2.202	3.218
20[1]	1.000	1.000	1.000
25	0.615	0.484	0.349
30	0.391	0.248	0.134
35	0.255	0.134	0.056
40	0.171	0.076	0.025
45	0.118	0.044	0.012
50	0.083	0.027	0.006

[1] Reference temperature

temperatures for R0 and R50 (23°C between R25 and R0 and 18°C between R25 and R50) were similar to the differences in their T_gs (26.5°C between R25 and R0 and 20.4°C between R25 and R50). It was observed that ${C_1}^0$ and ${C_2}^0$were very similar for R0, R25 and R50 when the curves overlapped. This is to be expected as they have the same G' versus G'' relationship demonstrated by the Cole-Cole plot (Fig. 7).

The implications of these observations are interesting from a practical perspective. Let us consider the case where it is desired to have an epoxidized NR having a particular dynamic property at a temperature T_{ref}. This may be achieved by shifting the mastercurves for the dynamic properties of NR by a horizontal multiplication factor (x_{r}) to a new frequency range so that the desired modulus at the required frequencies is obtained. Then, the change required in the T_g of NR can be calculated, and hence the epoxidation level required to obtain the dynamic properties under the desired conditions. Knowledge of the original three (before the application of x_{r}) shift factors (a_{T1}, a_{T2} and a_{T3}) and their respective temperatures (T_1, T_2 and T_3) is required to form three simultaneous

equations to solve for T_0 and ${C_2}^0$. It should be noted that T_0 is reference temperature for the NR master curve shifted by x_r, whereas T_ref is the reference temperature for the ENR curve i.e. the temperature at which the desired properties are required.

$$\alpha = \log x_\mathrm{r}\, a_{T1} = -\frac{{C_1}^0(T_1 - T_0)}{{C_2}^0 + T_1 - T_0} \tag{8}$$

$$\beta = \log x_\mathrm{r}\, a_{T2} = -\frac{{C_1}^0(T_2 - T_0)}{{C_2}^0 + T_2 - T_0} \tag{9}$$

$$\gamma = \log x_\mathrm{r}\, a_{T3} = -\frac{{C_1}^0(T_3 - T_0)}{{C_2}^0 + T_3 - T_0} \tag{10}$$

which leads to:

$$T_0 = \frac{\alpha\gamma T_2(T_3 - T_1) + \beta\gamma T_1(T_2 - T_3) + \alpha\beta T_3(T_1 - T_2)}{\alpha\gamma(T_3 - T_1) + \beta\gamma(T_2 - T_3) + \alpha\beta(T_1 - T_2)} \tag{11}$$

$${C_2}^0 = \frac{(\alpha - \beta)(T_1 - T_0)(T_2 - T_0)}{\beta(T_1 - T_0) - \alpha(T_2 - T_0)} \tag{12}$$

Alternatively, if T_s of the original polymer (NR) is known, then the following equation can be used instead of Eq. (12):

$${C_2}^0 = 101.6 + T_0 - T_s\,. \tag{13}$$

As mentioned earlier, the viscoelastic coefficients for overlapping NR and ENR compounds were found to be the same. The T_g of the ENR compound which gives the desired properties at T_ref can therefore be found:

$$T_\mathrm{g} = 101.6 + T_\mathrm{ref} - 50\text{°C} - {C_2}^0\,. \tag{14}$$

For example, using x_r as 0.06 (shifting R0 to match R25), T_1, T_2 and T_3 as -40°C, -35°C and -30°C, and a_{T1}, a_{T2} and a_{T3} as 31552, 7787 and 2232, the T_g for R25 is calculated, using Eqs. (11, 12 and 14) to be -48.5°C.

Another way of visualizing this data is to use a nomogram (Fig. 10). This nomogram has been constructed from the data for R0, but it is generalised to apply to any ENR compounds with known

T_g. The generalisation is approximate, but useful for design purposes. It could be employed in two ways.

The first is estimation of the modulus at different temperatures and frequencies. For example, if one needs to know the properties of a rubber at 10000 Hz and T_g+65 then, from the right-hand vertical axis 10000 Hz is chosen. This line is followed until the T_g+65 line is reached. The horizontal axis value at the point (~200000 Hz) is the corresponding frequency for T_g+90 (or the 20°C reference temperature of R0) and where the G' and G'' curves intersect this vertical line are the corresponding values for this frequency and temperature. The value of G' is ~2 MPa and G'' is ~3 MPa. T_g+65 is approximately 20°C for R25, so the figures for G' and G'' can be confirmed by comparing with Figs. 8 and 9. The second is to choose a suitable ENR compound based on desiring particular values of G' (or G'') at a particular frequency and temperature. To achieve this, a horizontal line is drawn from the desired frequency and a vertical line through the desired value of G'. The point of the intersection gives an estimate of the temperature above T_g at which these properties could be achieved. From the knowledge of the temperature for the application the T_g, and therefore the level of epoxidation can be estimated.

3.5 Application of 5-Parameter Fractional Derivative Pritz Model

The 5-parameter fractional derivative model by Pritz, referred here to as the 5-parameter fractional model, is the generalization of the conventional viscoelastic Zener model [17]. This model has been developed and used successfully to fit experimental data on some polymeric damping materials, especially over a wide frequency range [23]. It is also known that the model describes the asymmetrical broadening peak of the loss factor and the low increment of dynamic modulus at high frequencies [17]. However, in this paper the model is fitted to the experimental data at low- and medium frequencies only because the dynamic mechanical analysis was not performed at low enough temperatures to go well below the glass transition temperature for natural rubber. It is show in this part of the paper that the model satisfies the dynamic properties of natural rubber with different epoxidation levels over a wide frequency range.

The differential equation for the 5-parameter fractional model is [17]:

$$\sigma(t) + \tau^{\beta}\frac{\mathrm{d}^{\beta}}{\mathrm{d}t^{\beta}}\sigma(t) = G_0\varepsilon(t) + G_0\tau^{\beta}\frac{\mathrm{d}^{\beta}}{\mathrm{d}t^{\beta}}\varepsilon(t) + (G_\infty - G_0)\tau^{\alpha}\frac{\mathrm{d}^{\alpha}}{\mathrm{d}t^{\alpha}}\varepsilon(t). \quad (15)$$

This equation has five parameters, G_0, G_∞, α, β and τ which describe the dynamic behaviour of the material over a broad frequency range. The parameters G_0 and G_∞ are the low-frequency and high-frequency storage moduli, respectively. α is the parameter that determines the rate of change in the real and imaginary parts of the dynamic modulus in the low frequency range, i.e. below the

peak in the loss factor. The parameter β is the correction to the conventional 4-parameter fractional derivative Zener model that controls the asymmetry of the loss peak and the high-frequency behaviour of the real and imaginary parts of the dynamic modulus. The parameter τ is the relaxation time that controls the position of the peak in the loss factor.

The complex modulus for the 5-parameter fractional model is derived in the form of the following equation (Eq. 38 in ref. [17])

$$\bar{G}(\omega) = G_0 \; + \; G_0(d-1)\frac{(i\omega\tau)^{\alpha}}{1 \; + \; (i\omega\tau)^{\beta}} \; , \tag{16}$$

where

$$d = \frac{G_\infty}{G_0} \tag{17}$$

and the normalized frequency is

$$\omega_n = \omega\tau. \tag{18}$$

In this work the values for the 5-parameter fractional model were determined directly from the experimental master curves. Since no dynamic properties data were obtained at the low temperatures below the glass transition temperature, the minimization analysis

$$F(\boldsymbol{x}) = \sum_{n=1}^{N} |\bar{G}^{exp}(\omega_n, \boldsymbol{x}) - \bar{G}^{th}(\omega_n, \boldsymbol{x})| \rightarrow \min \, , \tag{19}$$

was carried out to invert the five parameters by fitting the predicted values of complex modulus, $\bar{G}^{th}(\omega_n, \boldsymbol{x})$, to the experimental data, $\bar{G}^{exp}(\omega_n, \boldsymbol{x})$, obtained at the frequencies ω_n. The design variable vector in Eq. (19) is $\boldsymbol{x} = \{G_0, G_\infty, \alpha, \beta, \tau\}$. The inverted values of the five parameters are shown in Table 5.

The predictions were performed for the inverted values of the five parameters and the results were compared with the experimental master curves. The results for the storage modulus and the loss modulus of R0, R25 and R50 rubbers are shown in Figs. 11 and 12. The master curves for the storage modulus suggest that there is a good correlation between the experimented and predicted results along the frequency range. The experimental master curves and that predicted by the 5-parameter fractional model are almost identical. The loss modulus of the rubbers exhibits similar behaviour by showing a good agreement from the top to middle part of the master curves (at and

Table 5
Optimized parameter values calculated for the 5-parameter fractional model.

Rubber	G_0 (Pa)	G_∞ (Pa)	α	β	τ (s)	d
R0	5.73 x 10^5	1.11 x 10^9	0.6828	0.6826	1.59 x 10^{-10}	1940
R25	5.84 x 10^5	4.03 x 10^8	0.7412	0.7388	1.78 x 10^{-8}	690
R50	6.60 x 10^5	3.21 x 10^8	0.7726	0.6926	9.95 x 10^{-7}	486

around the loss peak). However, as the frequency decreases, the disagreement between the data and the predictions becomes more pronounced. This disagreement may lead to considerable design errors if this model is used to predict the dynamic behaviour of the natural rubber that well above the glass transition temperature or for $\omega_n < 1$. Above this frequency range, the model accuracy is high with the maximum relative error being 5-8% for the storage modulus and 4-9% for the loss modulus. This observation suggests that the model proposed can provide a close agreement to the experimental master curves below the glass transition temperature or above $\omega_n > 1$.

4. Conclusions

Three types of rubber with different epoxidation levels: SMR-CV60 (0 mol%), ENR-25 (25 mol%), and ENR-50 (50 mol%) were the focus of this study. The master curves for their dynamic properties were constructed based on the time-temperature equivalence principle using Williams-Landel-Ferry (WLF) relationship for amorphous polymers.

Cole-Cole plots for all three vulcanizates fall on a single curve regardless of the level of epoxidation suggesting that the epoxidation does not influence the relationship between the storage modulus and loss modulus, but merely shifts the master curves for natural rubber along the frequency axis.

The results obtained in this work provide the basis for determining the optimal epoxidation level to achieve specific dynamic property requirements over a range of temperature and frequencies. A nomogram has been constructed for predicting the appropriate epoxidation level for such purposes. In addition, the 5-parameter fractional model for the dynamic properties of natural rubber with different epoxidation levels has been fitted to the experimental data. This model can fit well the experimentally obtained master curves with the maximum relative error of 4-9%.

Acknowledgements

The authors would like to express their appreciation to the Malaysian Rubber Board for providing the financial support during the period in which this research work was carried out. Sincere thanks

are also expressed to Leslie Morton, Charlie Forge and Colin Hull for their assistance throughout this work.

References

[1] J.E. Davey, M.J.R. Loadman, A chemical demonstration of the randomness of epoxidation of natural rubber, British Polymer Journal, 16 (1984) 134-138.
[2] S. Cook, P.S. Brown, J. Patel, A. Kepas-Suwara, Ekoprena™: A polymer for high performance passenger tyre treads, Malaysian Rubber Board Technical ReportHertford, United Kingdom, 2008.
[3] P. Intharapat, A. Kongnoo, K. Kateungngan, The potential of chicken eggshell waste as a bio-filler filled epoxidized natural rubber (ENR) composite and its properties, Journal of Polymers and the Environment, 21 (2013) 245-258.
[4] P.K. Chattopadhyay, S. Praveen, N. Chandra Das, S. Chattopadhyay, Contribution of organomodified clay on hybrid microstructures and properties of epoxidized natural rubber-based nanocomposites, Polymer Engineering & Science, 53 (2013) 923-930.
[5] I.R. Gelling, Modification of natural rubber latex with peracetic acid, Rubber Chemistry and Technology, 58 (1985) 86-96.
[6] Z.A. Nasir, U.S. Ishiaku, Z.A.M. Ishak, Determination of optimum blending conditions for poly(vinyl chloride)/epoxidized natural rubber blends, Journal of Applied Polymer Science, 47 (1993) 951-959.
[7] Z. Mohamad, H. Ismail, R. Chantara Thevy, Characterization of epoxidized natural rubber/ethylene vinyl acetate (ENR-50/EVA) blend: effect of blend ratio, Journal of Applied Polymer Science, 99 (2006) 1504-1515.
[8] Y. Wang, Q. Wang, Y. Luo, J. Zhong, Y. Li, C. He, Z. Peng, Role of epoxidized natural rubber in dynamic mechanical properties of NR/ENR/silica composites, Advanced Materials Research, 415-417 (2011) 415-419.
[9] P. Zhang, G. Huang, L. Qu, Y. Nie, G. Weng, Study on the self-crosslinking behavior based on polychloroprene rubber and epoxidized natural rubber, Journal of Applied Polymer Science, 125 (2012) 1084-1090.
[10] R. Huang, X. Lu, J. Long, S. Wu, H. Jiang, Preparation and damping mechanism of EPDM/ENR damping material with wide temperature range, Gaofenzi Cailiao Kexue Yu Gongcheng/Polymeric Materials Science and Engineering, 32 (2016) 119-124.
[11] N. Yamada, S. Shoji, H. Sasaki, A. Nagatani, K. Yamaguchi, S. Kohjiya, A.S. Hashim, Developments of high performance vibration absorber from poly(vinyl chloride)/chlorinated polyethylene/epoxidized natural rubber blend, Journal of Applied Polymer Science, 71 (1999) 855-863.
[12] R.M.B. Fernandes, L.L.Y. Visconte, R.C.R. Nunes, Curing characteristics and aging properties of natural rubber/epoxidized natural rubber and cellulose II, International Journal of Polymeric Materials and Polymeric Biomaterials, 60 (2011) 351-364.
[13] S. Rooj, V. Thakur, U. Gohs, U. Wagenknecht, A.K. Bhowmick, G. Heinrich, In situ reactive compatibilization of polypropylene/epoxidized natural rubber blends by electron induced reactive processing: novel in-line mixing technology, Polymers for Advanced Technologies, 22 (2011) 2257-2263.
[14] Y. Wang, L. Liao, J. Zhong, D. He, K. Xu, C. Yang, Y. Luo, Z. Peng, The behavior of natural rubber-epoxidized natural rubber-silica composites based on wet masterbatch technique, Journal of Applied Polymer Science, 133 (2016).
[15] X. Lu, X. Li, Broad temperature and frequency range damping materials based on epoxidized natural rubber, Journal of Elastomers & Plastics, 46 (1) (2014) 84-95.

[16] H.R. Ahmadi, C. Metherell, A.H. Muhr, Noise reduction with rubber, Euro.Noise 92, I.O.A., Imperial College London, 1992.
[17] T. Pritz, Five-parameter fractional derivative model for polymeric damping materials, Journal of Sound and Vibration, 265 (2003) 935-952.
[18] M. Sjoberg, On dynamic properties of rubber isolators, Department of Vehicle Engineering, Royal Institute of Technology, Stockholm, 2002.
[19] M. Etchessahar, S. Sahraoui, L. Benyahia, J.F. Tassin, Frequency dependence of elastic properties of acoustic foams, The Journal of the Acoustical Society of America, 117 (2005) 1114-1121.
[20] H.R. Ahmadi, A.H. Muhr, Characterization of dynamic properties of rubber appropriate to noise and vibration control, Plastics and Rubber Institute, Rubber in Engineering Group, London, 1991.
[21] M.L. Williams, R.F. Landel, J.D. Ferry, The temperature dependence of relaxation mechanisms in amorphous polymers and other glass-forming liquids, Journal of the American Chemical Society, 77 (1955) 3701-3707.
[22] K.S. Cole, R.H. Cole, Dispersion and absorption in dielectrics I. Alternating current characteristics, The Journal of Chemical Physics, 9 (1941) 341-351.
[23] T. Pritz, Analysis of four-parameter fractional derivative model of real solid materials, Journal of Sound and Vibration, 195 (1996) 103-115.

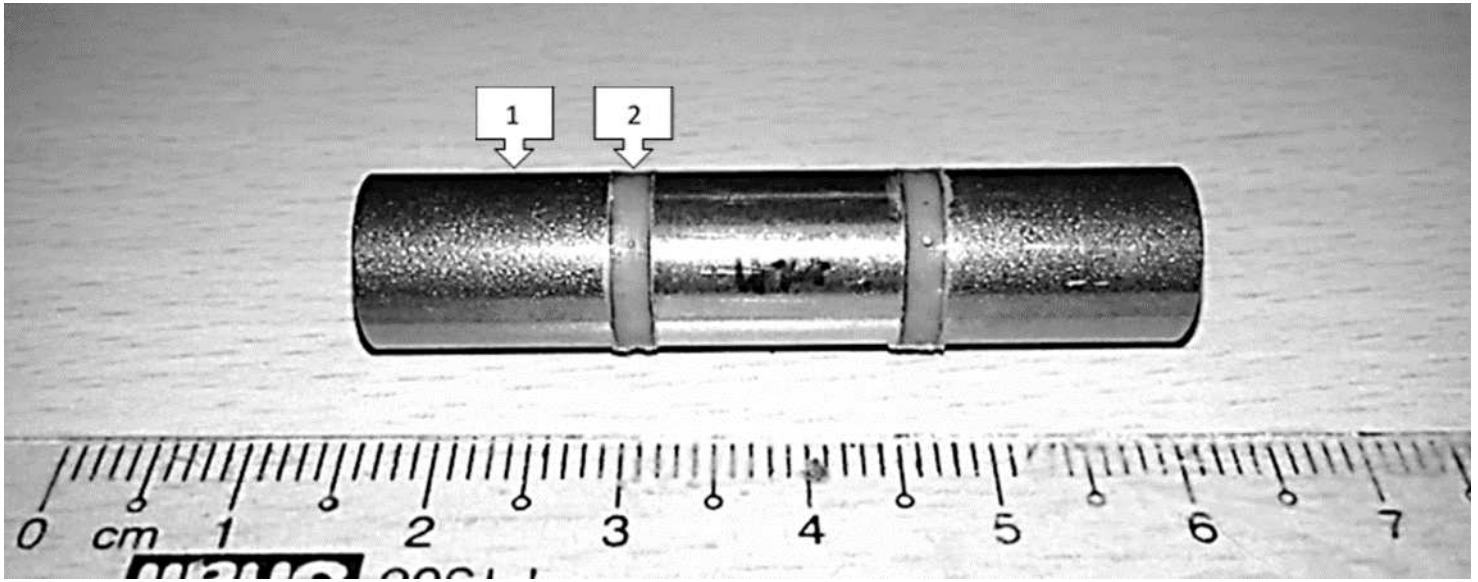

Fig. 1. A double bonded shear test piece. 1: stainless steel; 2: rubber.

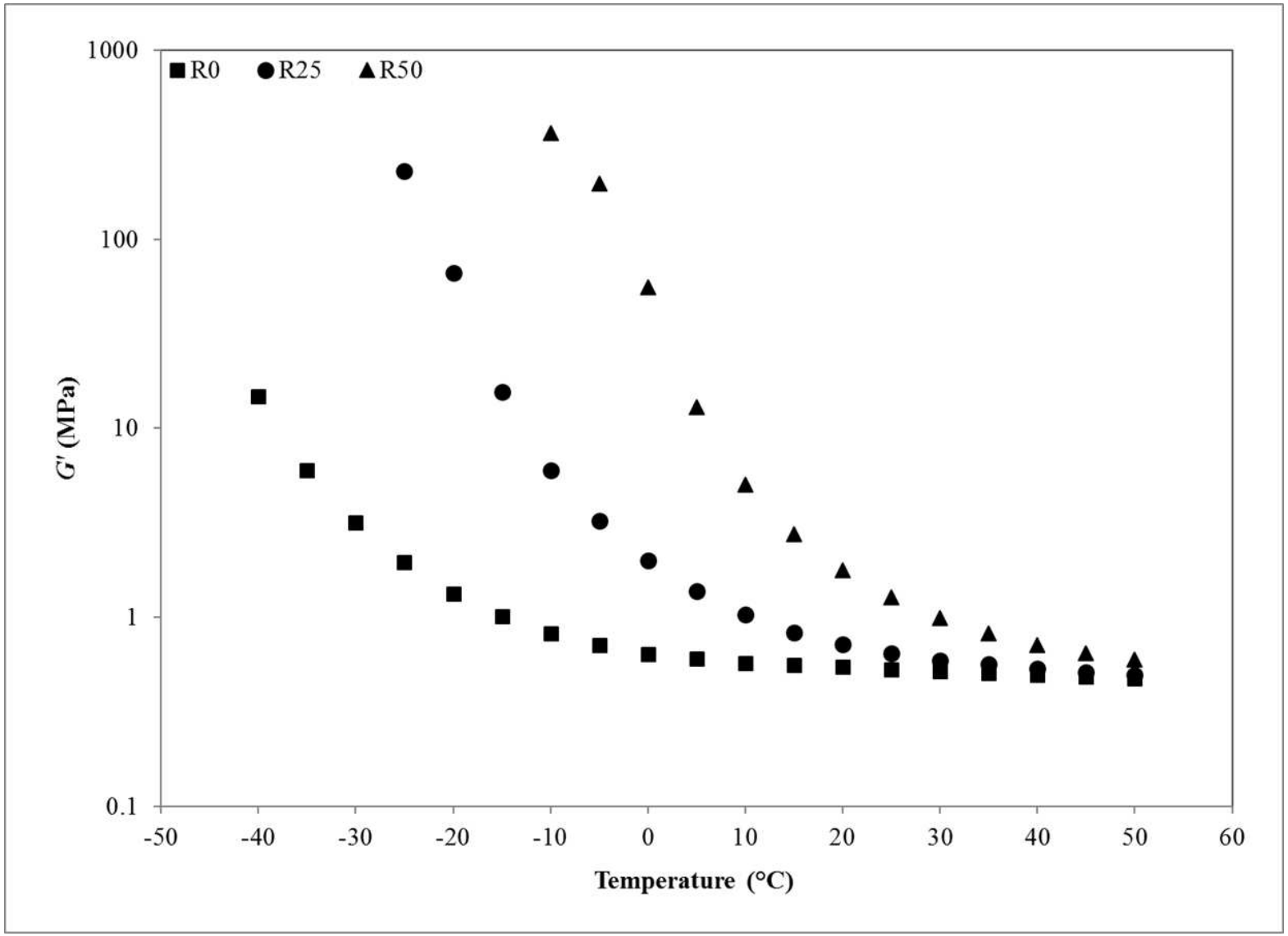

Fig. 2. The dependence of the storage modulus for R0, R25, and R50 rubbers as a function of temperature at 170Hz.

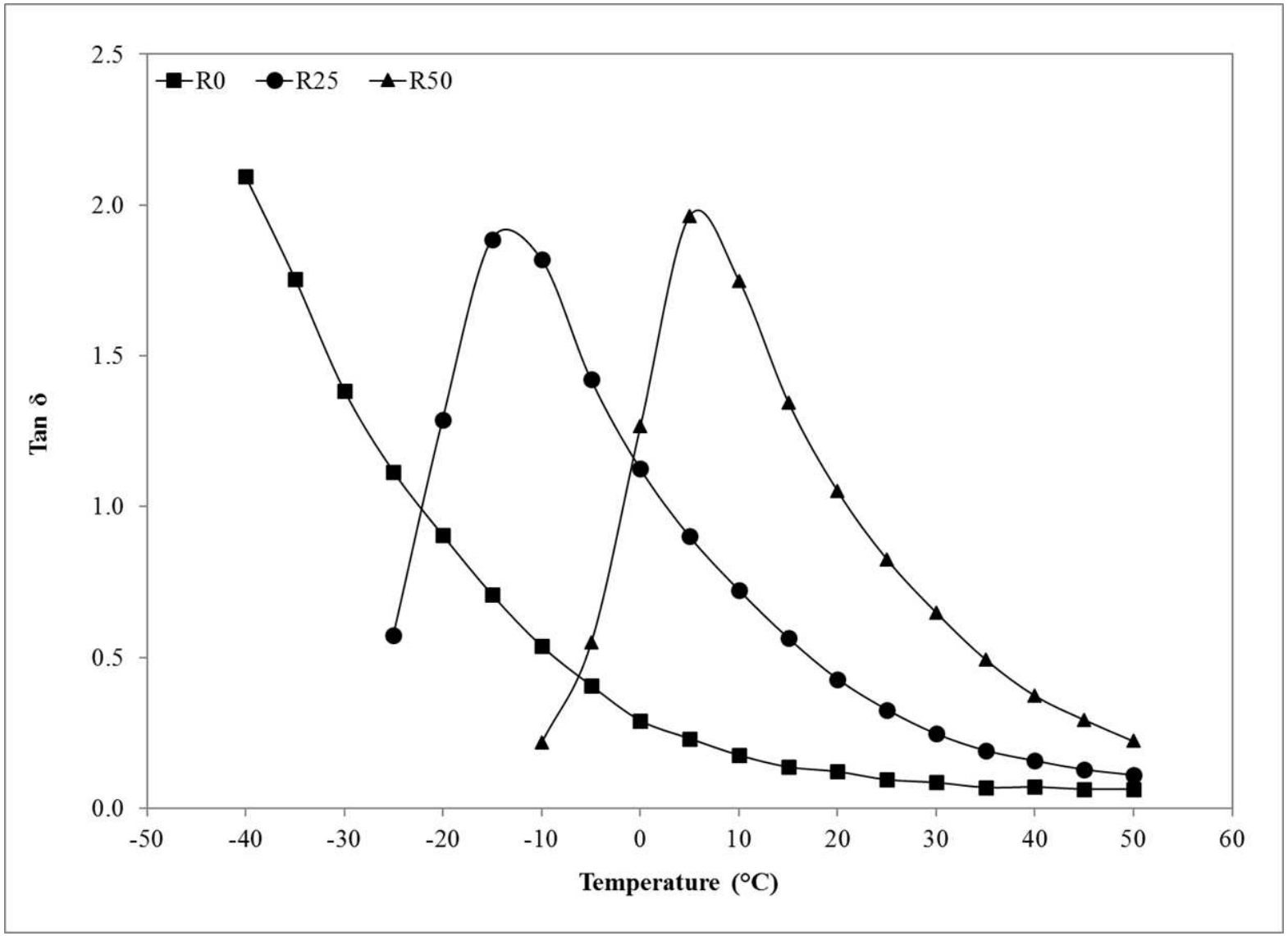

Fig. 3. The dependence of the loss factor (tan δ) for R0, R25 and R50 rubbers as a function of temperature at 170Hz.

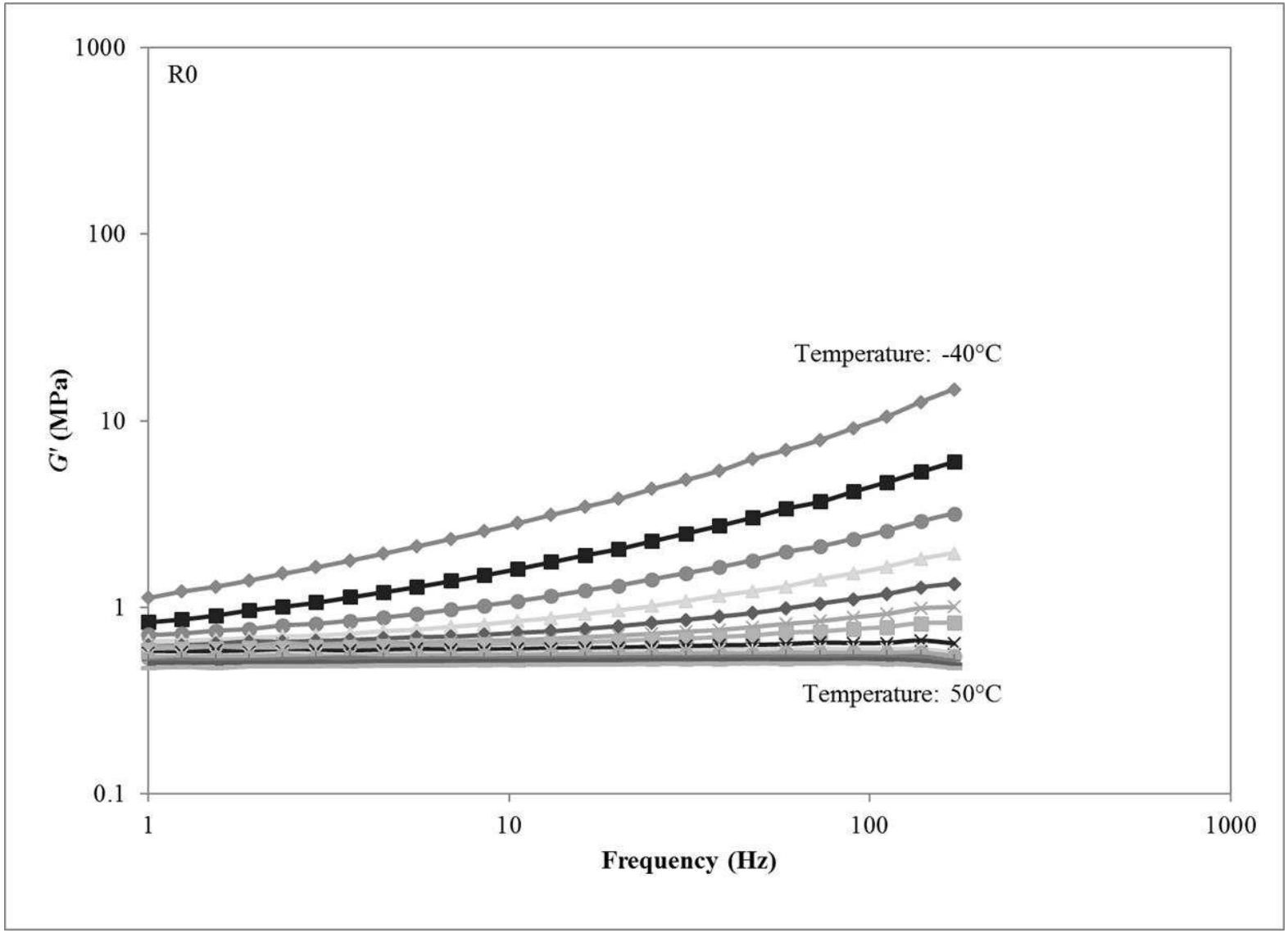

Fig. 4. The frequency dependence of the storage modulus of R0 rubber for a range of temperatures: -40°C to 50°C with 5°C interval.

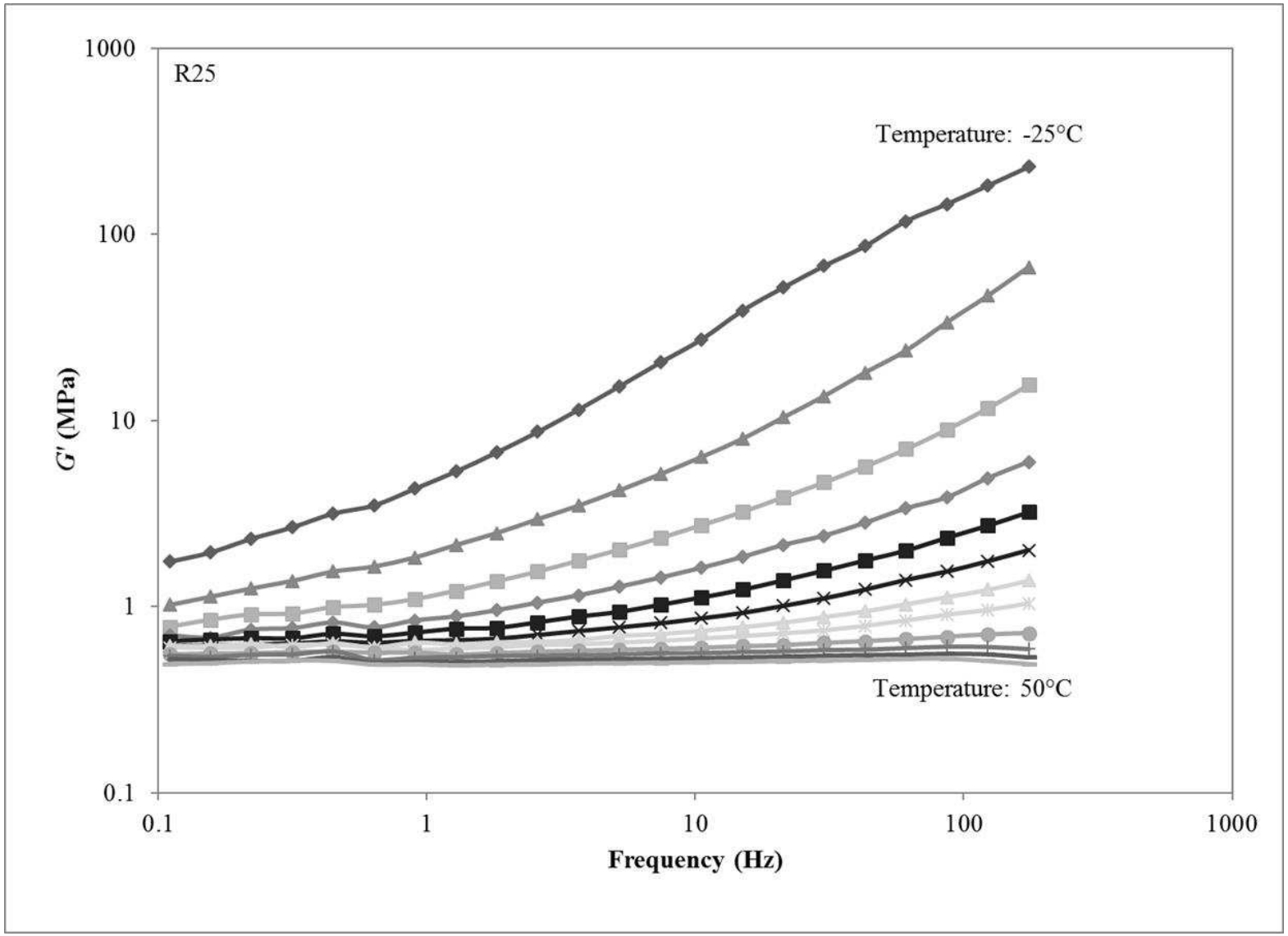

Fig. 5. The frequency dependence of the storage modulus of R25 rubber for a range of temperatures: -25°C to 50°C with 5°C interval.

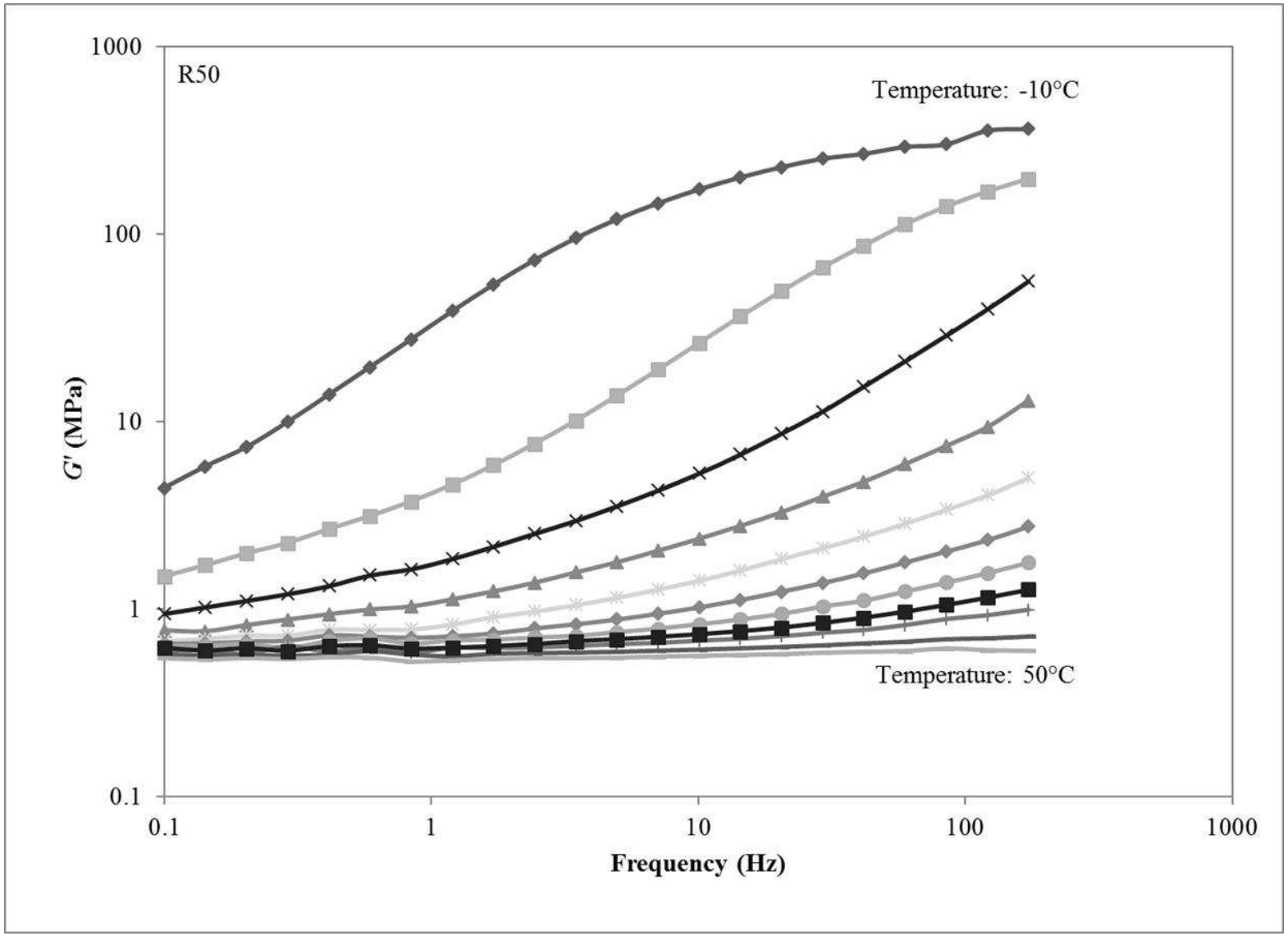

Fig. 6. The frequency dependence of the storage modulus of R50 rubber for a range of temperatures: -10°C to 50°C with 5°C interval.

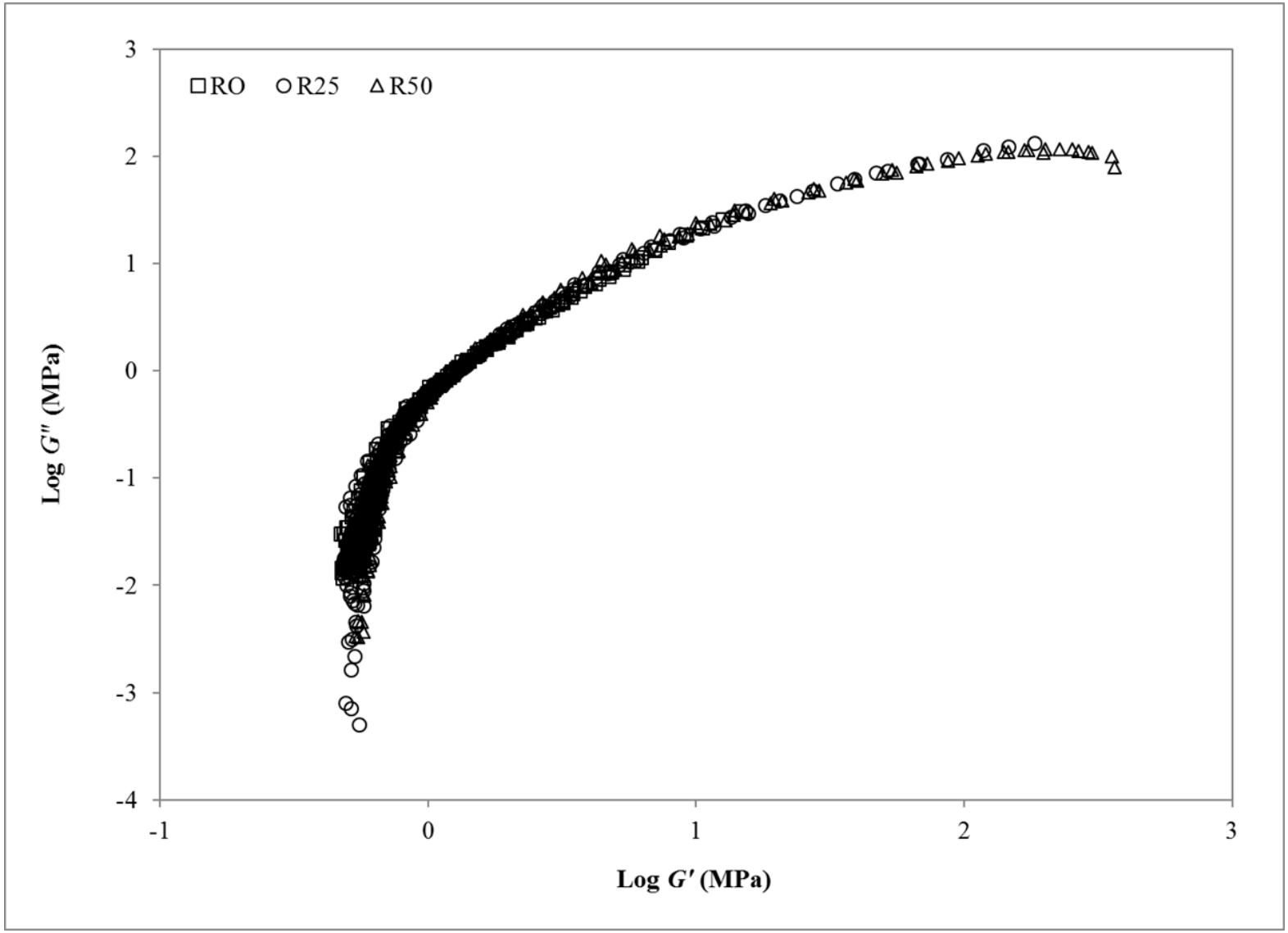

Fig. 7. The Cole-Cole plots for R0, R25 and R50 rubbers.

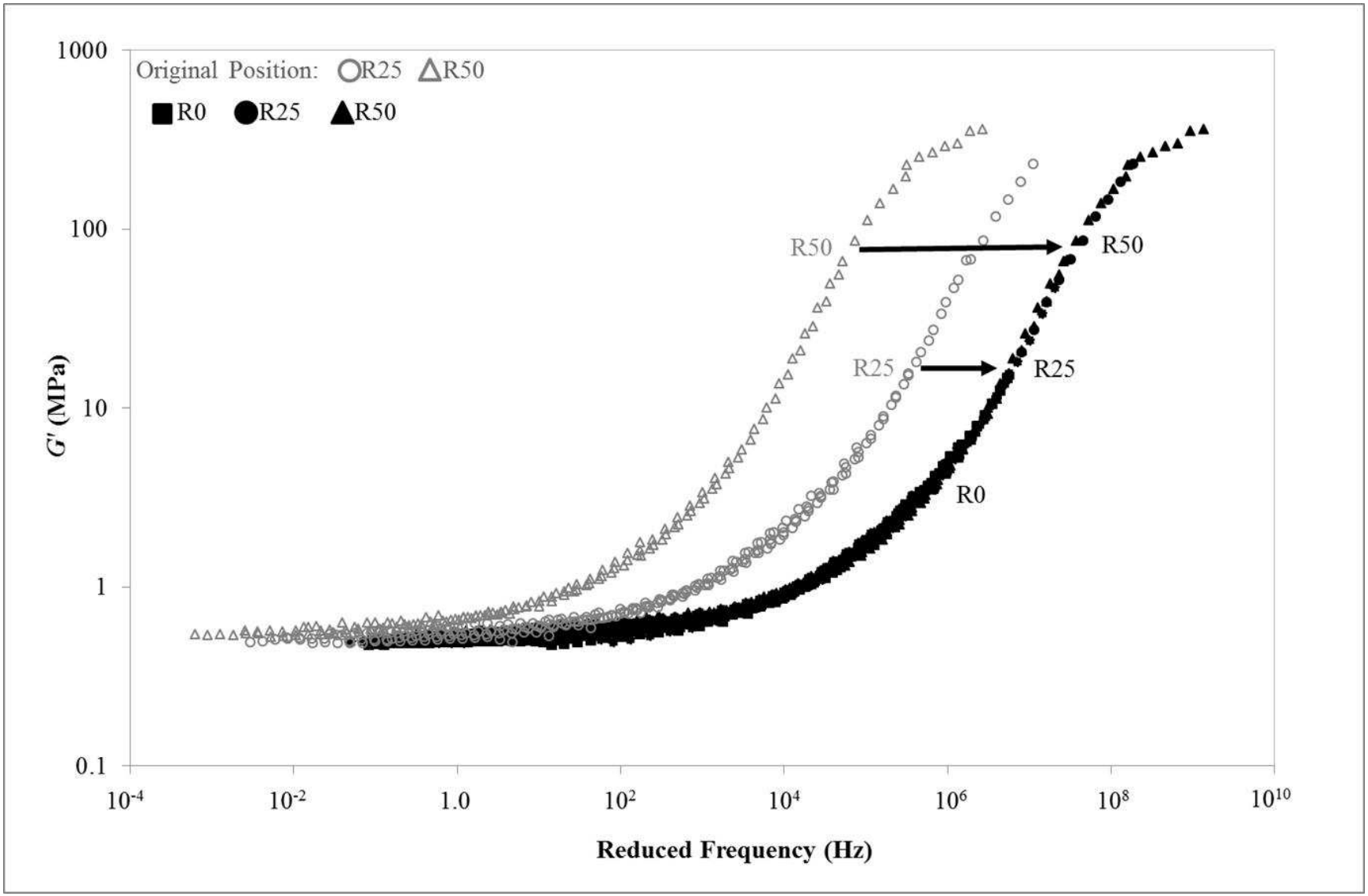

Fig. 8. A comparison of the master curves for the storage modulus of R0, R25 and R50 rubbers as a function of the reduced frequency.

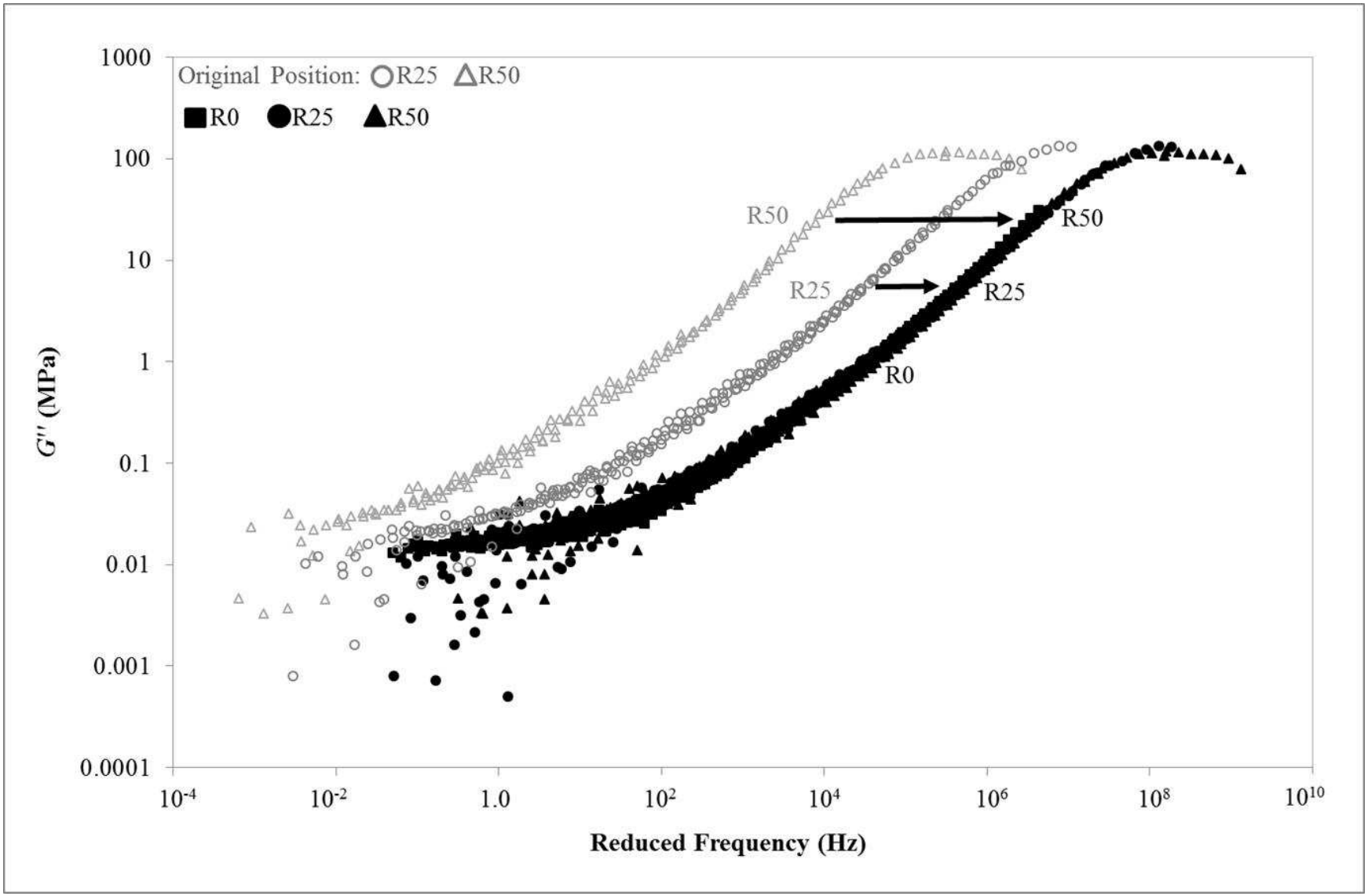

Fig. 9. A comparison of the master curves for the loss modulus of R0, R25 and R50 rubbers as a function of the reduced frequency.

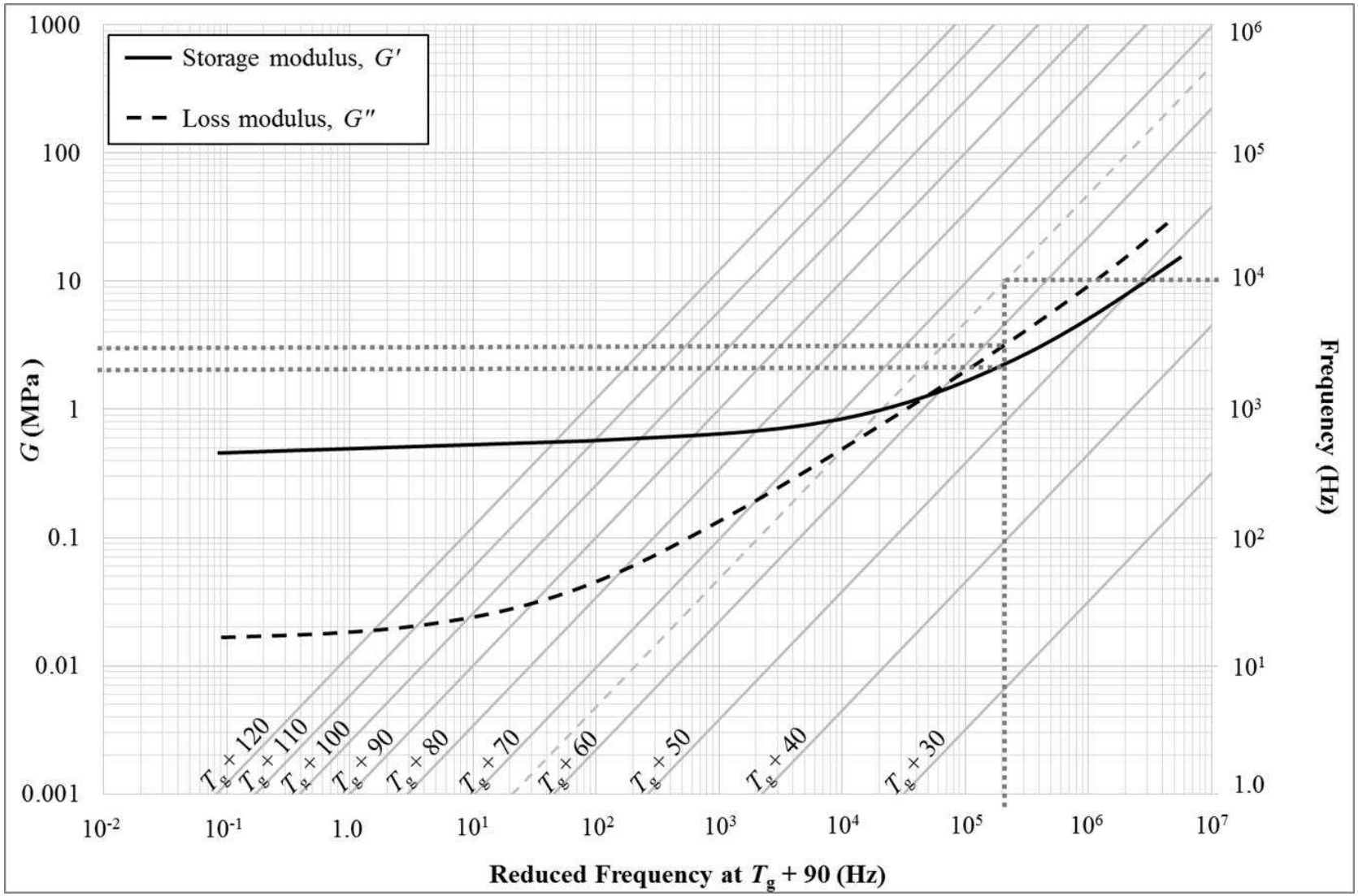

Fig. 10. A nomogram relating the reduced frequency to G' and G'' at different temperatures. The data is for NR (R0). The temperature in this nomogram has been standardised such that it is applicable to other ENR compounds with knowledge of the T_g.

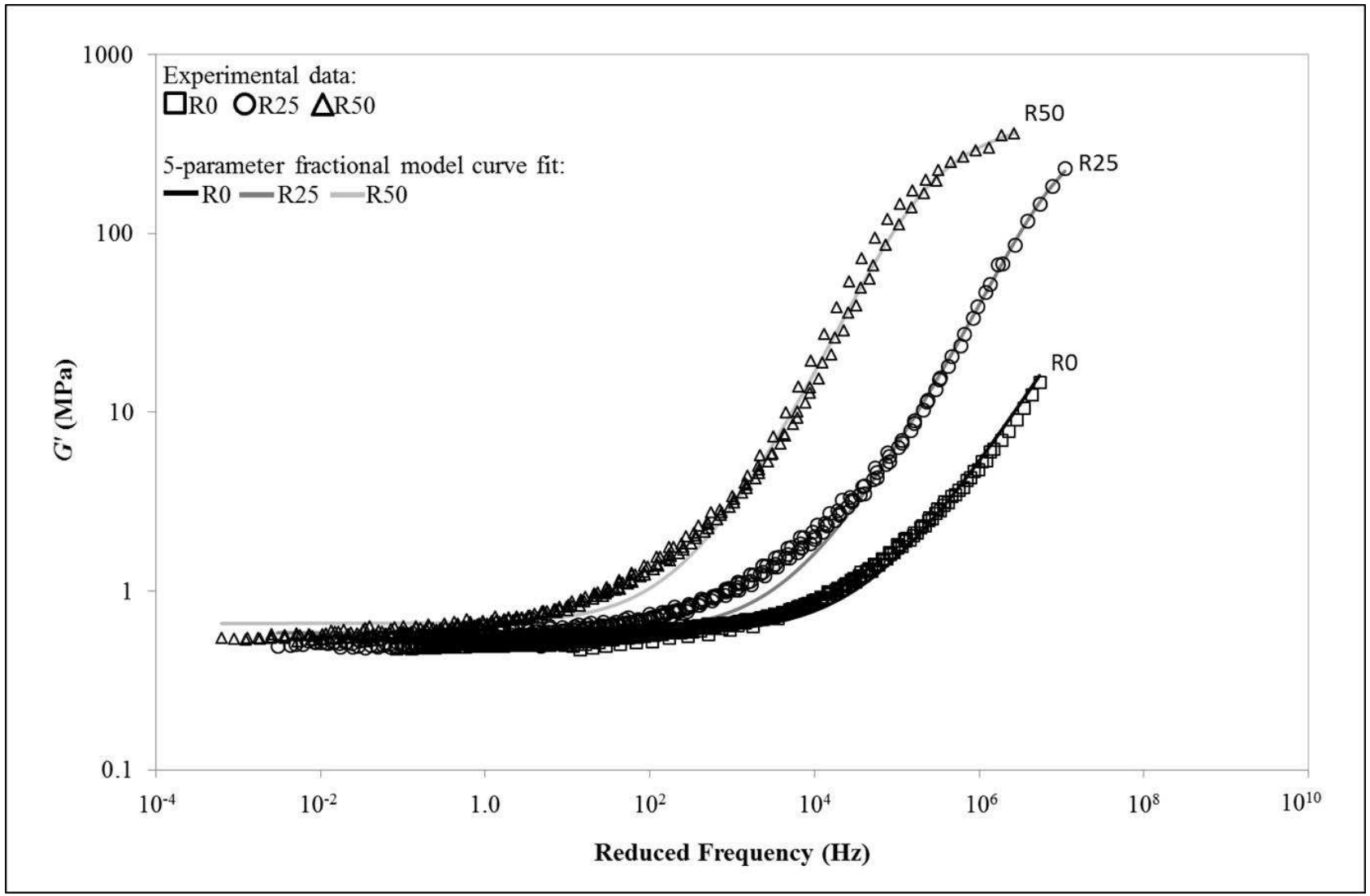

Fig. 11. A comparison between the master curves and predictions from the 5-parameter fractional model for the storage modulus of R0, R25 and R50 rubbers as a function of the reduced frequency.

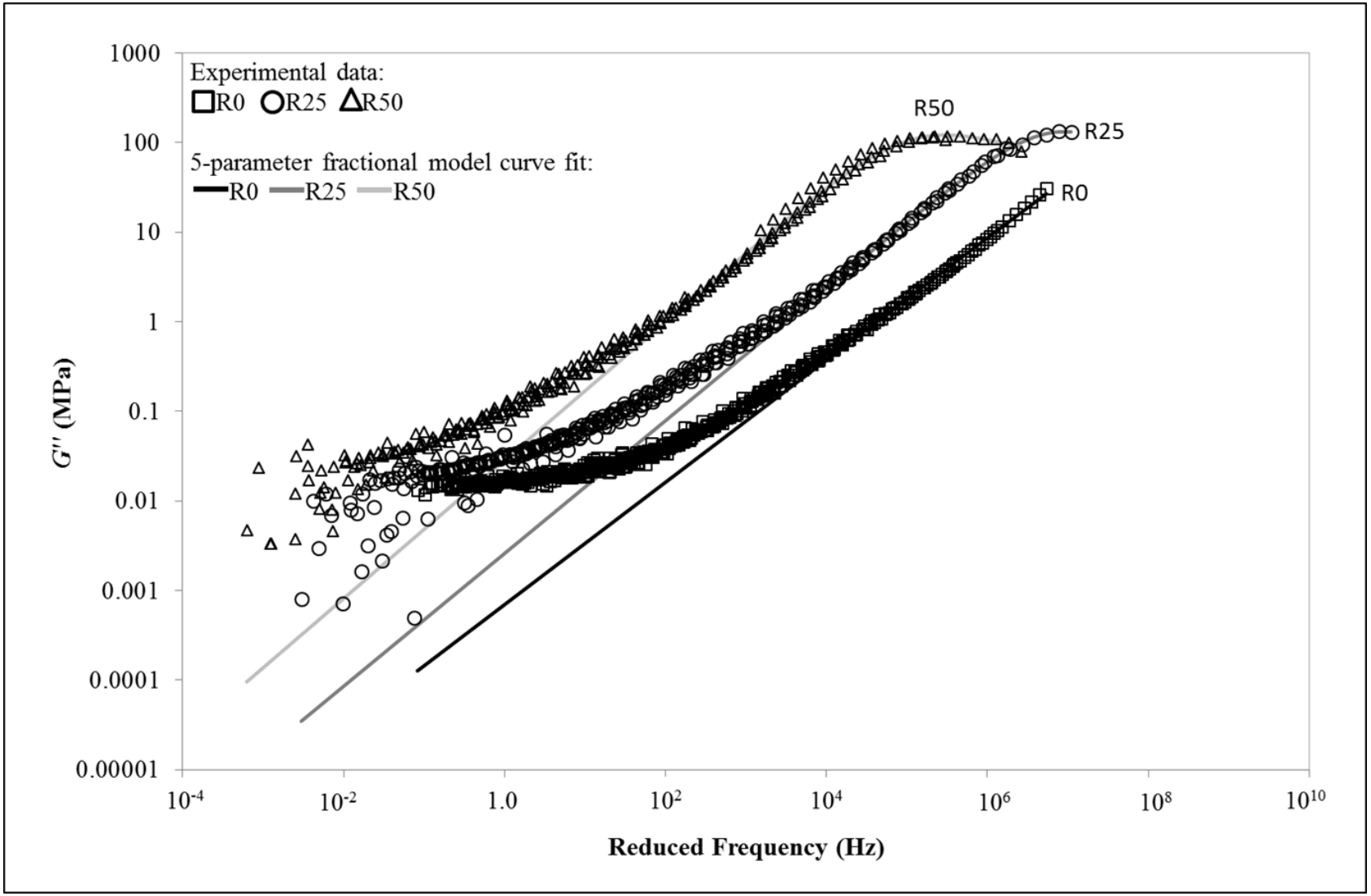

Fig. 12. A comparison between the master curves and predictions from the 5-parameter fractional model for the loss modulus of R0, R25 and R50 rubbers as a function of the reduced frequency.